Solid State Science and Technology, Vol. 32, No. 2 (2024) 121-134
https://doi.org/10.66514/ssst32-2-121-134

Influence of Hubbard *U* on the Structural and Electronic Properties of Pure and La-Doped ZnO

Muhd Aman Haikal Razali[1], Nur Ain Nabilah Mohamad Nor[1], Wan Hazeeq Azizi Wan Khairul Annuar[1], Mohd Hazrie Samat[2], Nur Hamizah Binti Mohd Zaki[1,2], Ahmad Firdaus Che Omar[2], Mohamad Fariz Mohamad Taib[1,2], Ferry Iskandar[4,5], Oskar Hasdinor Hassan[2,3,]*

[1]*Faculty of Applied Sciences, Universiti Teknologi MARA, 40450 Shah Alam Selangor, Malaysia*

[2]*Ionic Materials and Devices (iMADE), Institute of Science, Universiti Teknologi MARA, 40450 Shah Alam, Selangor, Malaysia*

[3]*Faculty of Arts and Design, Universiti Teknologi MARA, 40450 Shah Alam Selangor, Malaysia*

[4]*Department of Physics, Faculty of Mathematics and Natural Sciences, Institut Teknologi Bandung, Jl. Ganesha 10, 40132 Bandung, Indonesia*

[5]*Research Center for Nanosciences and Nanotechnology, Institut Teknologi Bandung Jl. Ganesha 10, 40132 Bandung, Indonesia*

** Corresponding author; email: amanhaikal5@gmail.com*

Received: 23 August 2024 / Accepted: 18 November 2024

ABSTRACT

The lattice parameters, average bond length, band structure and density of states (DOS) of pure ZnO and La-doped ZnO were calculated using the density functional theory (DFT) with the addition of Hubbard *U* (DFT+U) correction method. Lanthanum, La is a *p*-type dopant that might be viewed as a practical method for improving a piezoelectric nanogenerator's performance. The calculated lattice parameters and volume of pure ZnO expanded after La doping which are $a=b$=3.251 Å, c=5.208 Å and V= 48.346 Å^3. The Zn-O bond length of La-doped ZnO is higher than that of pure ZnO which makes the La-doped ZnO having stronger bonding than pure ZnO. The calculated band gap of pure ZnO was 3.415 eV and for La-doped ZnO, the band gap shows an increases to 3.457 eV. The calculated band gap approaches the experimental band gap with the implementation of Hubbard *U* at U_d at Zn and La sites and U_p at O sites. The density of states (DOS) of both pure ZnO and La-doped ZnO were conducted to determine the contribution of *s*, *p* and *d* orbitals that appear in the minimum conduction band and maximum valence band. As a result, we believe that our findings will be useful in understanding the doping impact in ZnO and will motivate further theoretical research.

Keywords: Density functional theory; electronic properties; La-doped ZnO; Hubbard *U*; structural properties; ZnO

INTRODUCTION

Zinc oxide (ZnO) is a II-VI compound semiconductor that has a wide direct band gap of around 3.3 to 3.4 eV and exhibits large exciton bonding energy (60 meV) at ambient temperature [1]. Because of its semiconductor properties, ZnO can be used in a variety of technological applications such as piezoelectric [2], gas sensor [3], light-emitting diodes [4], photocatalyst [5] and others.

Nowadays, computational method is an important part of materials research since they can solve and provide a detailed explanation of the structural and electronic properties of the materials. Generalize gradient approximation (GGA) and local density approximation (LDA) methods from various software programmes were used to evaluate structural and electronic properties of materials [6-9]. For pure ZnO, some researches have been performed the calculations based on the standard density functional theory (DFT) and the band gap energy obtained shows a range of value between 0.6 eV and 0.9 eV [6,7,10,11] which is an underestimate compared to the experimental energy band gap (3.4 eV) [12]. This is because the energy band gap for larger electronic *d* and *f* orbital systems was calculated inaccurately. For a better result on the electronic localization of *d* and *f* electrons and to improve the calculated energy band gap, several revised XC approximations, such as DFT+U, hybrid functional, GW approximation and DMFT, have been presented in the previous research [12]. In the calculation of the energy band gap of ZnO, the hybrid functionals (PBE0, HSE06, and sX) proved to be more accurate. However, hybrid functionals are known to have a greater computational cost and longer to solve the problem [13]. In the computation of structure, elastic constant, energy band gap, and electronic localization of 3d orbitals, the less expensive and more popular semiempirical GGA+U functional applied to ZnO has been reported to be more accurate [14]. Furthermore, the DFT+U method is appropriate and commonly employed in more complicated or large-scale systems of materials such as larger supercell structures, applications for substitution/doping, defects, and surface analyses [15].

ZnO has the potential to be a piezoelectric material that has attracted interest due to its high piezoelectricity and high level of biocompatibility. Many researchers have chosen to improve ZnO's piezoelectric property using various doping and interface techniques. Doping is one of the most basic methods for modifying the band gap and lattice parameters, which affect the piezoelectric output. Moreover, Yang Bai [16] states that materials with a wider band gap are perfect for piezoelectric applications. Impurity doping of ZnO has recently received a lot of attention [17] and is a useful method to increase the band gap. Previous research showed that the dopants from transition metal groups such as silver (Ag), aluminum (Al), molybdenum (Mo) and tin (Sn) doped with ZnO obtained band gap energies of 2.878 eV, 3.201 eV, 3.312 eV and 3.190 eV, respectively [18-20]. It was also reported that doping of group-I elements such as lithium (Li) and cerium (Ce) in ZnO also produced small band gap than rare-earth group which are 3.20 eV, 0.66 eV [21, 22]. The properties of ZnO can also be improved by doping with a rare earth metal element which is a special dopant with a particular electronic structure [23]. Achehboune et al. study on the electronic properties of both erbium-doped ZnO and ytterbium-doped ZnO. They determined the band gap of the doping crystal structure with the addition of Hubbard *U* at 3.290 eV and 3.250 eV [6,10]. Besides, Mohamed et al. study on the effect of gadolinium (Gd)

doping on on the structural, optical, and magnetic properties of ZnO based diluted magnetic semiconductor nanorods stated that the band gap of Gd-doped ZnO produced are 3.26 eV [8]. In previous research, Chen et al. have used the spin-coating process to create La-doped ZnO films with different La doping concentrations by using the sol-gel method. The band gap of La-doped ZnO films increases linearly from 3.270 to 3.326 eV [5]. In addition, Deng et al. [24] studied the effect of La doping on the electronic structure and optical properties of ZnO via standard DFT and obtained a band gap of 0.837 eV. Meanwhile, the same conclusions were also drawn in another work [25]. In addition, a previous study by Kang et al. showed that the La-doping could improve the output piezoelectric performance of ZnO since the band gap of La-doping is greater than that of pure ZnO [1].

In this work, we focused on theoretical studies of pure and La-doped ZnO using a first-principle study based on the density functional theory (DFT). The standard DFT method which uses XC functionals from LDA, GGA and GGA-PBEsol obtained the underestimated band gap energy. However, there is no further understanding of how to apply Hubbard *U* to the properties of La-doped ZnO. Hence, here we performed a detailed analysis on the structural parameters, the average bond length, band structure and density of states of pure ZnO and La-doped ZnO with a focus on the DFT and DFT+U methods.

COMPUTATIONAL METHOD

The first-principle study was performed with the Cambridge Serial Total Energy Package (CASTEP) [26] code which is based on the density functional theory (DFT) with implementation of Hubbard *U* (DFT+U) via a plane wave pseudopotential method. The exchange-correlation (XC) functional known as local density approximation by Ceperley and Alder as parametrized by Perdew and Zunger (LDA-CAPZ) [27, 28] and generalized gradient approximation of Perdew-Burke-Ernzerhof (GGA-PBE) [29] and Perdew-Burke-Ernzerhof for solids (GGA-PBEsol) [30] were used in the calculation. The ZnO was hexagonal wurtzite which corresponds to the P63mc space group. The core region and valence electrons of the atoms in the 2×2×2 supercell of pure ZnO and La-doped ZnO are described by LDA and GGA functionals. The valence-electron configuration for Zn, O and La atoms is chosen as Zn-$3d^{10}s^2$, O-$2s^2p^4$ and La-$5s^25p^65d^16s^2$, respectively. The numerical integration of the Brillouin zone for Monkhorst-Pack *k*-point sampling is performed using 5×5×4 for pure ZnO and 6×6×1 for La-doped ZnO, respectively, with the cut-off energy of the plane wave is 380 eV. In a 2×2×2 supercell of ZnO, the percentage of dopant (La) is 6.25% where La is substituted at a rate of one atom per 16 total atoms of Zn. The energy change, maximum force, maximum stress, and maximum displacement convergence threshold parameters were set at 1.0×10^{-5} eV/atom, 0.03 eV/Å, 0.05 GPa, and 0.001 Å, respectively. In this study, the doping was accomplished by simply substituting a La atom for the Zn atom in the ZnO crystal structure. The Hubbard *U* method is applied to predict the accuracy of structural properties and to improve the calculated results of pure ZnO and La-doped ZnO since the DFT method produced an underestimated results in electronic properties. Thus, the calculated structural and electronic properties of the pure ZnO and La-doped ZnO in this work using DFT and DFT+U with the strong effective on-site Coulomb repulsion among the localized *d* and *p*-state were described according to the following formalism:

$$E_{DFT+U} = E_{DFT} \frac{(U-J)}{2} \sum_{\sigma} Tr(\rho^{\sigma} - \rho^{\sigma}\rho^{\sigma}) \quad (1)$$

RESULTS AND DISCUSSION

Structural Properties

The structural parameters are computed to explain the physical properties of pure ZnO and La-doped ZnO. The crystal structure of La-doped ZnO is shown in Figure 1. The La-doped ZnO was constructed by replacing one of the Zn atoms with La atom. The 2×2×2 supercell of ZnO consists of 16 Zn atom and 16 O atom. There are 16 different positions of Zn that can be substituted by La. Thus, the most stable position of La was investigated by calculating the formation energy of La doping in ZnO structure at different doping positions as shown in Figure 2. According to the law of energy conversion, formation energy is the difference between the energy of the systems after and before the replacement. The substitutional reaction may occur at the position where the formation energy is lower. The formation energy formula in this work refers to the formalism published by Van de Walle et al. [31]. The following formulas are used to compute the formation energy, E_f:

$$E_f = E_{La:ZnO} + E_{Zn} - (E_{ZnO} + E_{La}) \quad (2)$$

where $E_{La:ZnO}$ is the total energy of La-doped ZnO, E_{ZnO} is the total energy of pure ZnO and E_{La} and E_{Zn} represent the energy of single La atom and Zn atom, respectively. La doping in ZnO is most efficient at the P4 position since it has the lowest formation energy. The position at P.4 is more stable than other position with E_f= -30000.76543874 eV. As a result, this structure has been used in the calculations for the structural and electrical properties of La-doped ZnO.

The calculated lattice parameters and volume of both pure ZnO and La-doped ZnO from LDA-CAPZ, GGA-PBE and GGA-PBEsol functionals compared with the experimental data were listed in Table 1. For pure ZnO, the calculated lattice parameters from GGA-PBEsol functional with the values of *a*=*b*=3.245 Å and *c*=5.234 Å are very close to the determined lattice parameters by previous experiment result [32]. When the La atom is substituted for the Zn atom, it can be seen clearly that the calculated lattice parameters, *a*=*b*=3.250 Å and *c*=5.240 Å from LDA-CAPZ functional are close to the experimental data [33]. Besides, it was found that the lattice parameters and volume of the La-doped ZnO were larger than those of pure ZnO. This is because the ionic diameter (radius) of the La^{3+} ion (1.22 Å) is greater than that of the Zn^{+} ion (0.74 Å) [33]. As a result, it can be said that even though La-doping affected the values of the lattice parameters, the crystal system (hexagonal) and space group (*P63mc*) remained the same.

Based on the optimized cell structure, the average bond lengths of pure ZnO and La-doped ZnO were investigated and tabulated as in Table 2. The bond length of Zn-O increases from 1.980 Å to 1.991 Å after La atom replaces the Zn atom. This results from the difference in atomic radius between Zn and La. Since Zn has a smaller atomic radius than La, O atoms are spread out closer to La and form shorter Zn-O bonds as a result. Additionally, it should be noted that there is higher population of La-O bonds than Zn-O bonds.

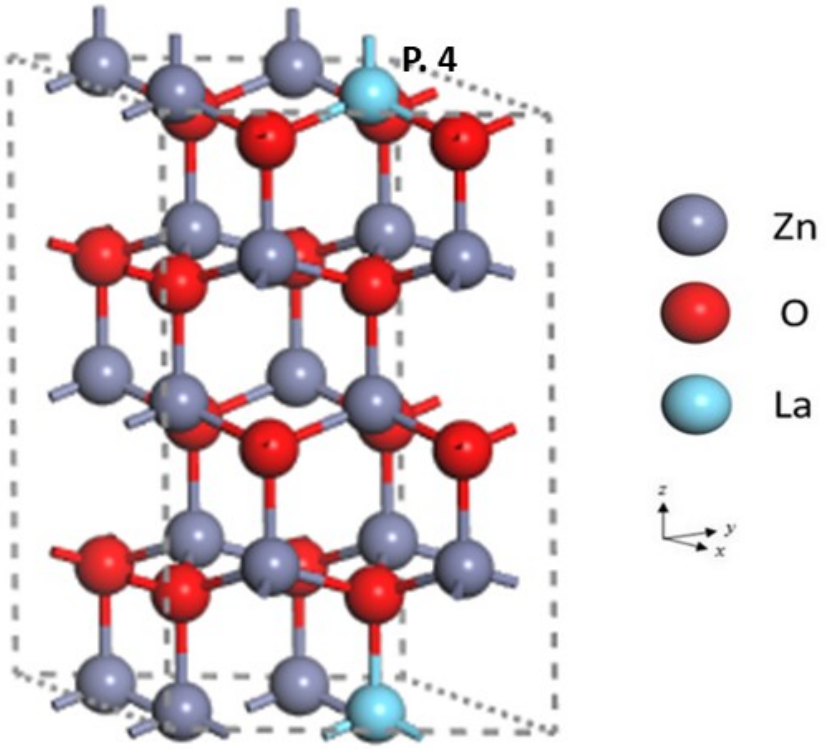

Figure 1. Crystal structure of 2×2×2 supercell of La-doped ZnO (P. is referred as position)

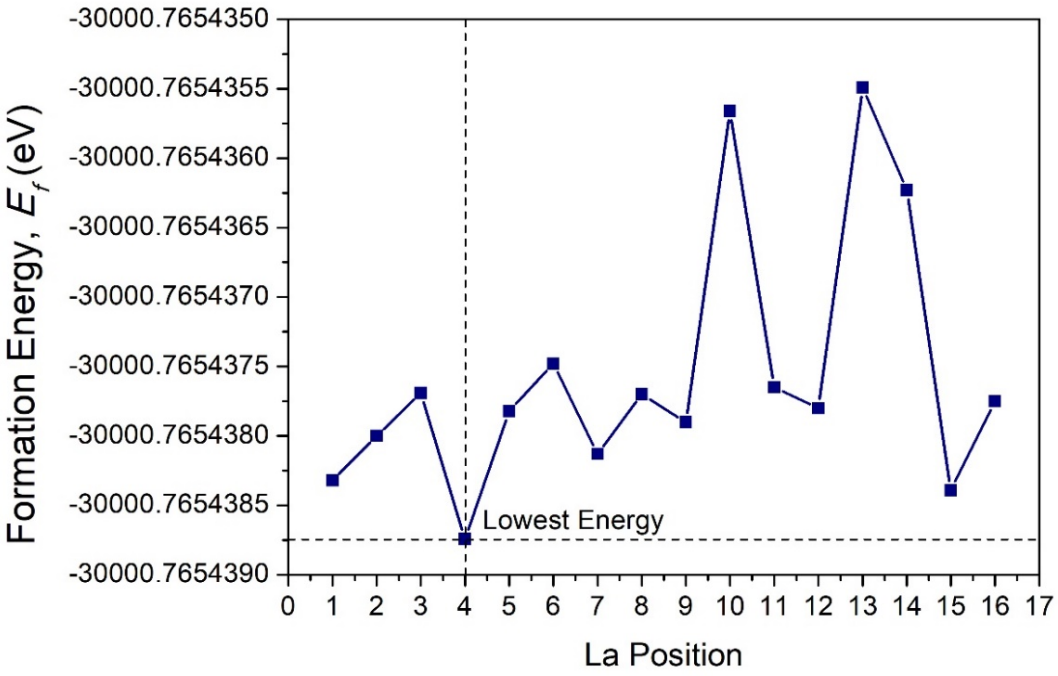

Figure 2. Formation energy of La-doped ZnO in different La positions

Table 1. Structural parameters of pure ZnO and La-doped ZnO by using LDA-CAPZ, GGA-PBE and GGA-PBEsol functionals compared to the experimental data

	Materials	Method	$a=b$ (Å)	c (Å)	V (Å^3)	Ref.
Calculated	Pure ZnO	LDA-CAPZ	3.190	5.160	45.485	This work
		GGA-PBE	3.289	5.305	49.693	This work
		GGA-PBEsol	**3.245**	**5.234**	**47.726**	This work
		LDA	3.189	5.237	46.181	[8]
		GGA-PBEsol	3.257	5.337	49.024	[8]
		GGA-PBE-HSE06	3.262	5.212	-	[9]
	La-doped ZnO	**LDA-CAPZ**	**3.250**	**5.240**	**48.346**	This work
		GGA-PBE	3.347	5.364	53.090	This work
		GGA-PBEsol	3.301	5.290	50.643	This work
		GGA-PBE	3.285	5.294	-	[34]
Experiment	Pure ZnO	XRD	3.251	5.208	48.023	[32]
	La-doped ZnO	XRD	3.250	5.206	47.610	[33]

Table 2. Average bond length for pure ZnO and La-doped ZnO

Bond	Pure ZnO (Å)	La-doped ZnO (Å)
Zn-O	1.980	1.991
O-O	-	2.933
La-O	-	2.265

Band structures

The band structures of pure ZnO as displayed in Figure 3(a) shows a direct band gap of about 0.618 eV at the symmetric *G* point which is lower than the experimental band gaps of 3.4 eV [35]. The underestimated value of the bandgap in pure ZnO is caused by weaknesses in LDA and GGA, which underestimate the binding energy in the *d*-state and cause an excess of hybridization with anion *p*-valence states. The DFT+U method tends to stabilize the localized *d*-state and *p*-state of the electron in a correlated system.

The calculations of the band gap of pure ZnO using value of U at the *d*-state of Zn, $U_{d,Zn}$, from 2 eV to 10 eV are shown in Figure 4(a). However, the highest $U_{d,Zn}$ at 10 eV presents a band gap of 1.108 eV which is still far from the experimental band

gap. According to the previous author, considering U at the p-state of O, $U_{p,O}$, has no effect on the total energy [36]. In fact, the band gap near the experimental was achieved by combining $U_{d,Zn}$ and $U_{p,O}$. Thus, the $U_{d,Zn}$ are set between 5 eV and 10 eV, while $U_{p,O}$ are set in the range of 5 eV to 10 eV. As a result, the energy band gap increased to 3.415 eV and slightly exceeded the experimental energy band gap (3.4 eV) after adding the U value in both the $U_{d,Zn}$ at 9 eV and $U_{p,O}$ at 8 eV as shown in Figure 3(b) and 4(b). Besides, the energy band gap of ZnO from our calculation is consistent and close to the other DFT+U results as shown in Table 3 [6, 7, 10, 11].

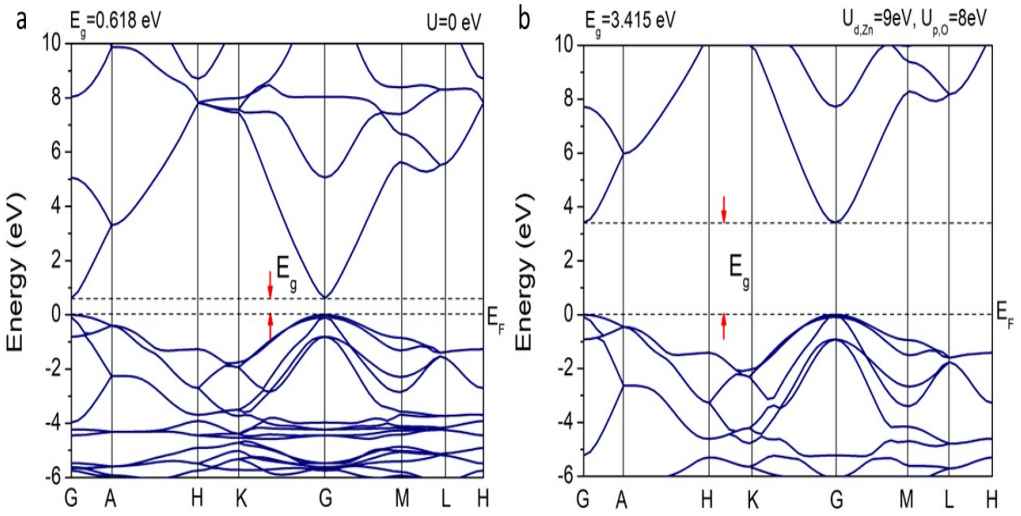

Figure 3. Band structure of (a) ZnO and (b) ZnO+U

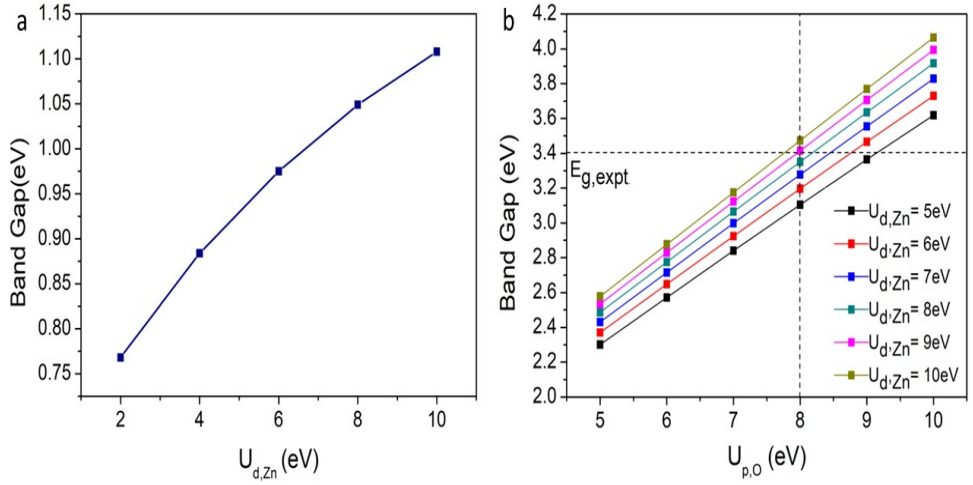

Figure 4. Relationship between (a) $U_{d,Zn}$ vs band gap for ZnO and (b) $U_{p,O}$ vs band gap of ZnO

The band structures of La-doped ZnO without Hubbard U correction method are shown in Figure 5(a). The calculated band gap of La-doped ZnO is 0.715 eV which is underestimated compared to the experimental band gap of 3.30 eV [5]. It is clearly seen that the band gap of La-doped ZnO is larger than that of pure ZnO which is consistent with the experimental band gap [5, 24]. For the La-doped ZnO with Hubbard U correction method, lanthanum (III) oxide (La_2O_3) calculation was used to determine the U value needed to add in the La atom. La_2O_3 has an experimental band gap of about 5.5 eV [37]. The calculated band gap of La_2O_3 from GGA-PBEsol functional is 3.662

eV which is lower than the experimental band gap. Therefore, the DFT+U method can be adopted. After varying the U value at the d-state of La, $U_{d,La}$, between 2 eV and 10 eV, the bandgap was far from the experimental data as presented in Figure 6(a). Thus, the U value was incorporated into the p-state of La, $U_{p,La}$, which varied it in the range of 2 eV to 10 eV while the La d-state, $U_{d,La}$, and the O p-state, $U_{p,O}$ were fixed at 2 eV and 8 eV, respectively (Figure 6(b)). The result from $U_{d,La}$ = 2 eV and $U_{p,La}$ = 6 eV values indicated that the energy band gap of La_2O_3 is increase to 5.449 eV which is close to the experimental band gap. The selected U values from the La_2O_3 structure were used to proceed with the calculation of the energy band gap for La-doped ZnO. In Figure 6(b), the calculation of La-doped ZnO with the implementation of selected U values ($U_{d,Zn}$ = 9 eV, $U_{d,La}$ = 2 eV, $U_{p,La}$ = 6 eV and $U_{p,O}$ = 8 eV) shows that the band gap energy is equivalent to 3.457 eV which is quite overestimated compared to the experimental result [5]. This result can be compared with other rare-earth elements results. For example, the previous researches from Achehboune et al. [6, 10] study on the Er-doped ZnO and Yb-doped ZnO, obtained band gap of the doping crystal structure with the inclusion of Hubbard U at 3.290 eV and 3.650 eV after doping with Er and Yb dopants, respectively, towards the Zn site.

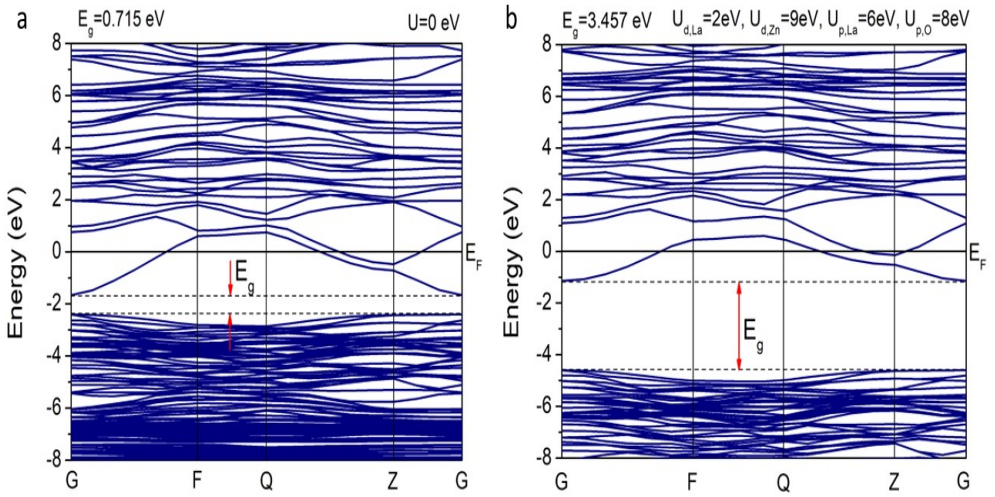

Figure 5. Band structure of (a) La-doped ZnO and (b) La-doped ZnO+U

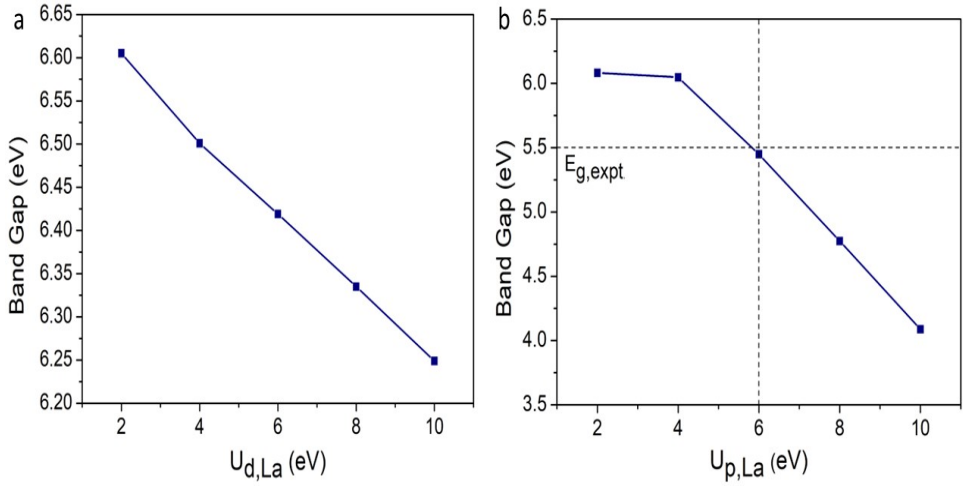

Figure 6. Relationship between (a) $U_{d,La}$ vs band gap for La-doped ZnO and (b) $U_{p,La}$ vs band gap of La-doped ZnO ($U_{d,La}$ and $U_{p,O}$ were fixed at 2 eV and 8 eV, respectively)

The doped La atoms cause a significant change in the energy band structure in the La doped ZnO system when compared to the pure ZnO. The electron states have degenerated and there are a lot of extra electrons in the bottom of the conduction band for La doped ZnO systems. Both the top of the valence band and the bottom of the conduction band shift in the direction of the lower energy level. However, variation extent of the former is much smaller than the latter one. Therefore, energy gap in ZnO with La-doping increases comparing to the pure ZnO as tabulate in Table 3.

Table 3. Energy bandgap of ZnO and La-doped ZnO by using DFT and DFT+U methods

Materials	Method	Energy band gap (eV)			References
		DFT	DFT+U	Experiment	
ZnO	GGA-PBEsol	0.618	3.415	-	This work
	GGA-PBE	0.740	3.380	-	[6]
	GGA-PBE	-	3.380	-	[10]
	LDA-CAPZ	0.795	3.097	-	[7]
	GGA-PBE	0.741	3.092	-	[7]
	GGA-PBEsol	0.622	3.102	-	[7]
	GGA-PW91	0.813	3.172	-	[11]
	UV-VIS Spectrocsopy	-	-	3.4	[38]
	X-ray Spectroscopy	-	-	3.3	[39]
La-doped ZnO	LDA-CAPZ	0.715	3.457	-	This work
	Sol-gel	-	-	3.3	[5]

Density of states (DOS)

Figures 7 and 8 show the partial density of state (PDOS) and total density of state (TDOS) for pure ZnO and ZnO+U, respectively. In the Figure 7, the valence band (VB) of pure ZnO mainly consist of contributions from O-2*p*, O-2*s* and Zn-3*d* states. The conduction band (CB) is formed mostly by Zn-4s state and a weak contribution of O-2*p* state was found. Based on Figure 8, applying Hubbard *U* at *d* and *p*-states (U_d+U_p) caused the Zn-3*d* and O-2*p* states at VB to shift towards the lower energy and Zn-4*s* and O-2*p* states at CB shifts toward higher energy level resulting in a widening of the band gap.

The partial density of state (PDOS) and total density of state (TDOS) of La-doped ZnO and La-doped ZnO+U are showed in Figures 9 and 10, respectively. When ZnO doped by La atom, it is clearly seen that the Fermi level shifts upward into the conduction band which is the so-called Burstein-Moss effect due to the surplus electrons by the doping of La on ZnO as shown in Figure 9. With the implemented of Hubbard *U* as illustrated in Figure 10, the contribution of Zn-3*d*, O-2*p*, O-2*s*, La-5*p* and La-6*s* shifts toward the lower energy valence band cause of opening band gap from E_g= 0.715 eV to E_g= 3.457 eV.

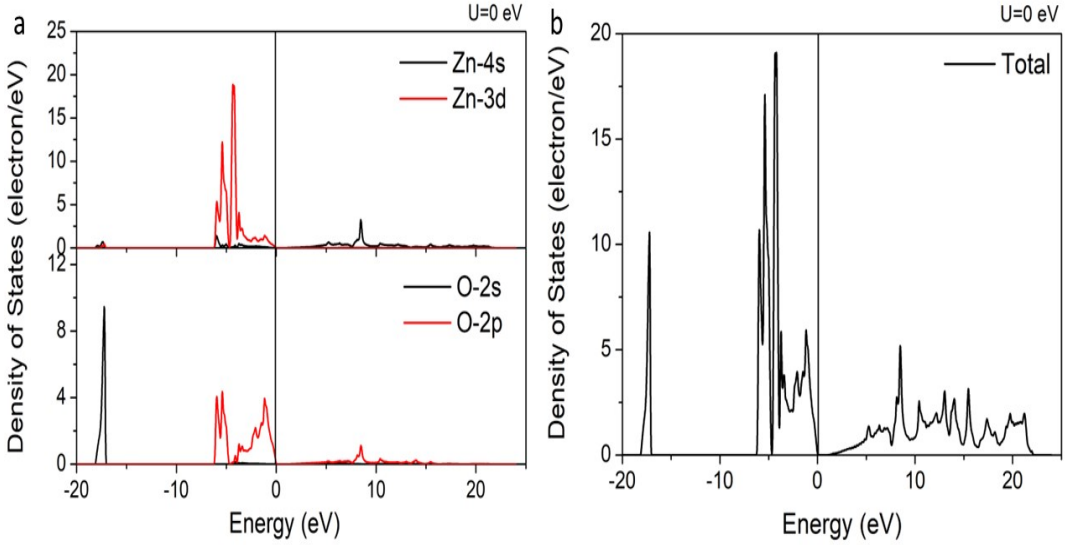

Figure 7. (a) PDOS of ZnO (b) DOS of ZnO

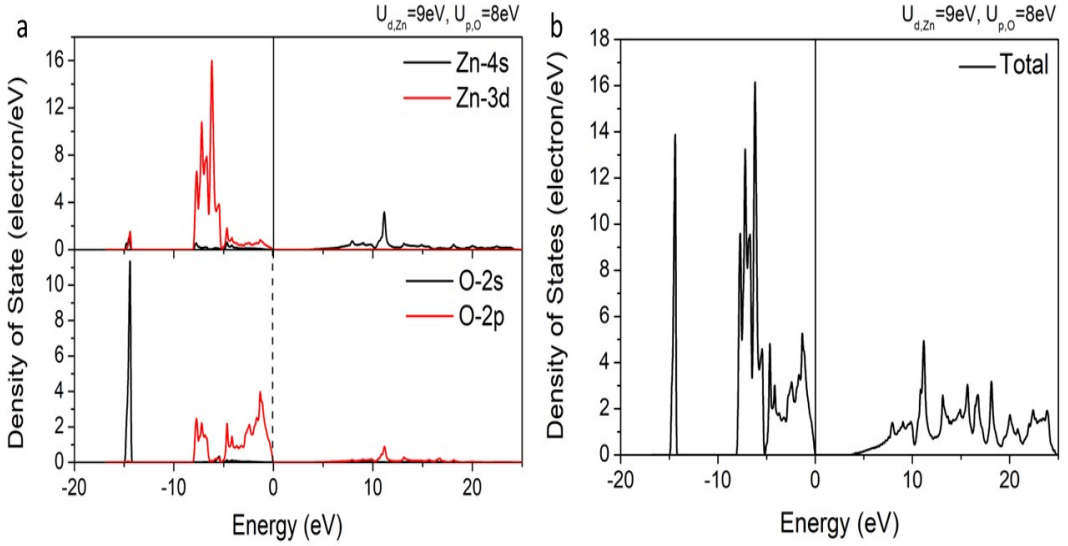

Figure 8. (a) PDOS of ZnO+U (b) DOS of ZnO+U

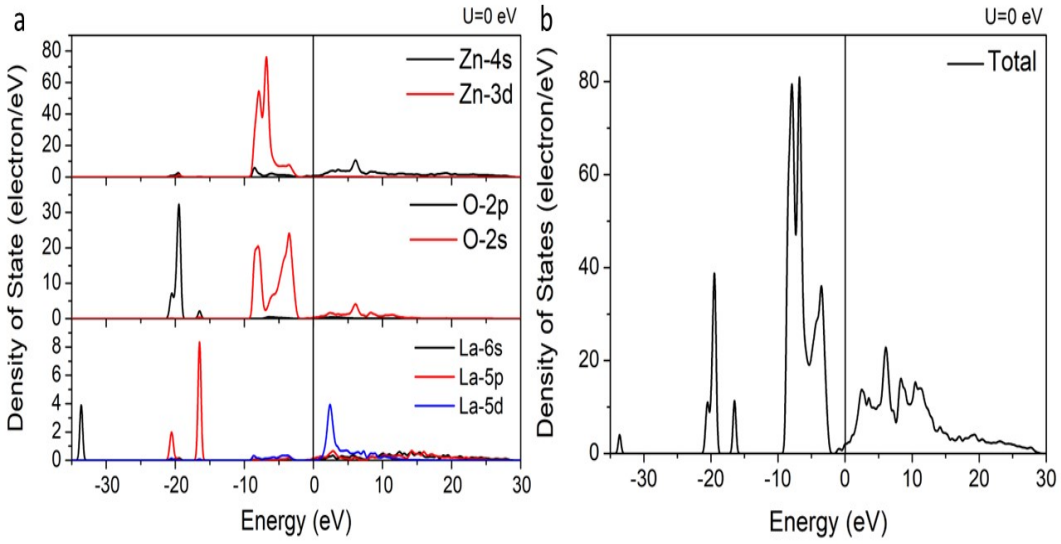

Figure 9. (a) PDOS of La-doped ZnO (b) DOS of La-doped ZnO

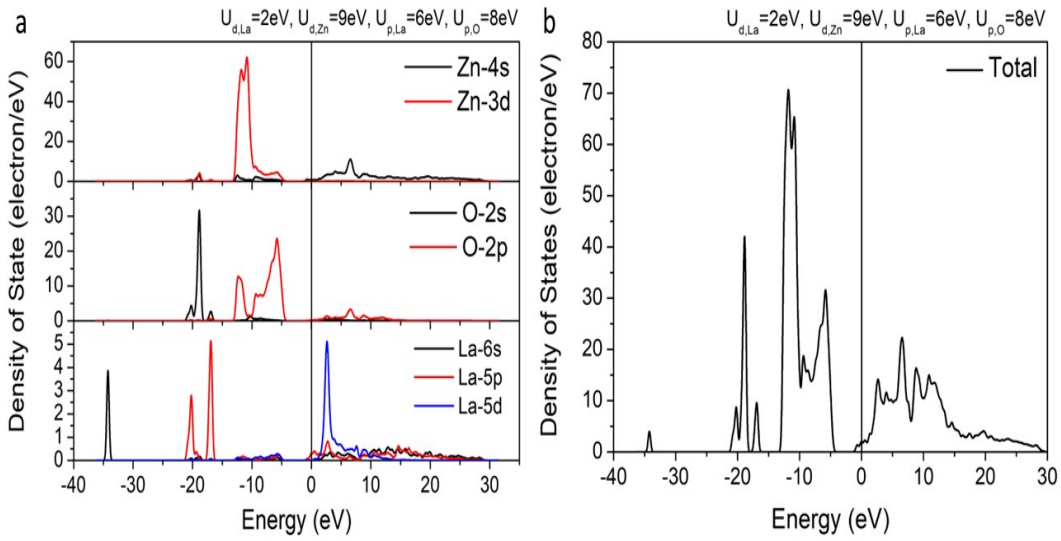

Figure 10. (a) PDOS of La-doped ZnO+U (b) DOS of La-doped ZnO+U

CONCLUSIONS

In this paper, based on the first-principle theory, the DFT+U method is used to calculate the effect of La doping on the structural and electronic properties of pure ZnO. For the structural properties, the lattice parameters and volume expanded when La was added to the ZnO materials. The La and O atoms on the ZnO have strong interactions and weak Zn-O bonds. The standard DFT calculation of the energy band gap of pure ZnO and La-doped ZnO produces an underestimated value compared to the experimental result. Thus, the Hubbard *U* correction method tends to maintain the electron's localised p and d-states in stable states. The band gap of pure ZnO increases from 3.415 eV to 3.457 eV after doping with the La atom. The electrons in the La orbit are transferred to the 2p orbit of the O atom. At the same time, 2p electrons from O atoms are transferred to Zn atoms, resulting in the positive charge of Zn atoms being reduced significantly. The Fermi energy level shifted up into the conduction band due to the surplus electrons caused by the participation of lanthanum. Thus, La-doped ZnO has the characteristics of a degenerate semiconductor and widens the energy gap of ZnO.

ACKNOWLEDGEMENTS

This work was supported by the Universiti Teknologi MARA under Geran Insentif Penyelidikan (600-RMC/GIP 5/3 (017/2022)). The authors would like to thank to Universiti Teknologi Mara (UiTM), Ionics, Materials and Devices (iMADE) Research Laboratory and Institute of Science (IOS) for their support in providing research facilities for this research.

REFERENCES

[1] L. Kang, H. An, J. Y. Park, M. H. Hong, S. Nahm, C. G. Lee (2019). La-doped p-type ZnO nanowire with enhanced piezoelectric performance for flexible nanogenerators, *Applied Surface Science* **475**, 969.

[2] P. Rajagopalan, P. Jakhar, I. A. Palani, V. Singh, S. J. Kim (2019). Elucidations on the effect of lanthanum doping in zno towards enhanced performance nanogenerators, *International Journal of Precision Engineering and Manufacturing-Green Technology* **7**, 77.
[3] W. Shen, Y. Zhao, C. Zhang (2005). The preparation of ZnO based gas-sensing thin films by ink-jet printing method, *Thin Solid Films* **483**, 382.
[4] H. H. Noriko Saito, T. Sekiguchi, N. Ohashi, I. Sakaguchi, K. Koumoto (2002). Low-temperature fabrication of light-emitting zinc oxide micropatterns using self-assembled monolayers, *Adv. Mater.* **14**, 418.
[5] J. T. Chen, J. Wang, F. Zhang, G. A. Zhang, Z. G. Wu, P. X. Yan (2008). The effect of La doping concentration on the properties of zinc oxide films prepared by the sol–gel method, *Journal of Crystal Growth* **310**, 2627.
[6] M. K. Mohamed Achehboune, I. Boukhoubza, I. Derkaoui, B. M. Mothudi, I. Zorkani, A. Jorio (2022). A DFT study on the electronic structure, magnetic and optical properties of Er doped ZnO: Effect of Er concentration and native defects, *Computational Condensed Matter* **31**, e00627.
[7] K. Harun, M. K. Yaakob, M. F. Mohamad Taib, B. Sahraoui, Z. A. Ahmad, A. A. Mohamad (2017) Efficient diagnostics of the electronic and optical properties of defective ZnO nanoparticles synthesized using the sol–gel method: experimental and theoretical studies, *Materials Research Express* **4**, 1.
[8] A.A. Mohamad, M.S. Hassan, M.K. Yaakob, M.F.M. Taib, F.W. Badrudin, O.H. Hassan, M.Z.A. Yahya (2017) First-principles calculation on electronic properties of zinc oxide by zinc–air system, *Journal of King Saud University - Engineering Sciences* **29**, 278.
[9] J.-H. Luo, Q. Liu, L.-N. Yang, Z.-Z. Sun, Z.-S. Li (2014). First-principles study of electronic structure and optical properties of (Zr–Al)-codoped ZnO, *Computational Materials Science* **82**, 70.
[10] M. K. Mohamed Achehboune, I. Boukhoubza, I. Derkaoui, Bakang Moses Mothudi, Izeddine Zorkani & Anouar Jorio (2021). Effect of Yb concentration on the structural, magnetic and optoelectronic properties of Yb doped ZnO, *Optical and Quantum Electronics* **53**, 1-14.
[11] H. Cao, P. Lu, N. Cai, X. Zhang, Z. Yu, T. Gao, S. Wang (2014). First-principles study on electronic and magnetic properties of (Mn,Fe)-codoped ZnO, *Journal of Magnetism and Magnetic Materials* **352**, 66.
[12] N. A. S. Kausar Harun, Bahri Deghfel, Muhamad Kamil Yaakob, Ahmad Azmin Mohamad (2020). DFT + U calculations for electronic, structural, and optical properties of ZnO wurtzite structure: A review, *Results in Physics* **16**, 102829.
[13] P. J. Hasnip, K. Refson, M. I. Probert, J. R. Yates, S. J. Clark, C. J. Pickard (2014). Density functional theory in the solid state, *Philos Trans A Math Phys Eng Sci.* **372**, 20130270.
[14] M.K.Yaakob, N.H. Hussin, M.F.M. Taib, T.I.T. Kudin, O.H. Hassan, A.M.M. Ali, M.Z.A. Yahya (2014). First Principles LDA+U Calculations for ZnO Materials, *Integrated Ferroelectrics* **155**, 15.
[15] L. Qiao, C. Chai, Y. Yang, X. Yu, C. Shi (2014). Strain effects on band structure of wurtzite ZnO: a GGA +Ustudy, *Journal of Semiconductors* **35**, 073004.
[16] Y. Bai (2021). Photoresponsive Piezoelectrics. *Frontiers in Materials* **8**.
[17] S. Y. Huang, S. Xu, J. W. Chai, Q. J. Cheng, J. D. Long, K. Ostrikov (2009). p-type doping of ZnO by means of high-density inductively coupled plasmas, *Materials Letters* **63**, 972.

[18] M. X. Zhaoyang Li, Xinli Li, Jiwen Li, Nannan Wang, Shengkang Zhang (2021). First principle study of electronic structure and optical properties of Mo doped ZnO with different concentrations, *Optik - International Journal for Light and Electron Optics* **228**, 166136.
[19] N. l. A. Slassi, Y. Ziat, Z. Zarhri, A. Fakhim Lamrani, E.K. Hlil, A. Benyoussef (2015). Ab initio study on the electronic, optical and electrical properties of Ti-, Sn- and Zr-doped ZnO, *Solid State Communications* **218**, 45.
[20] H. Chen, Y. Qu, L. Sun, J. Peng, J. Ding (2019). Band structures and optical properties of Ag and Al co-doped ZnO by experimental and theoretic calculation, *Physica E: Low-dimensional Systems and Nanostructures.* **114**, 113602.
[21] W. Hb, D. Wr, Z. B, M. Mj (2018). Li-doped ZnO sol-gel thin films: correlation between structural morphological and optical properties, *Journal of Textile Science & Engineering* **08**, 1000328.
[22] G. B. Z. Yun Geng Zhang, Yuan Xu Wang (2011). First-principles study of the electronic structure and optical properties of Ce-doped ZnO, *Journal of Applied Physics* **109**, 063510.
[23] R. N. Bhargava (1997). The role of impurity in doped nanocrystals, *Journal of Luminescence* **72-74**, 46.
[24] S. H. Deng, M. Y. Duan, M. Xu, L. He (2011). Effect of La doping on the electronic structure and optical properties of ZnO, *Physica B: Condensed Matter* **406**, 2314.
[25] X. Q. Liu, R. F. Zhang, Y. G. Su, X. J. Wang (2011). Study on the energy band structure of La Doped ZnO, *Advanced Materials Research* **233-235**, 2119.
[26] M. D. S. Stewart J. Clark, Chris J. Pickard, Phil J. Hasnip, Matt I. J. Probert, Keith Refson and Mike C. Payne (2005). First principles methods using CASTEP, *Zeitschrift für Kristallographie* **220**, 567.
[27] D. M. Ceperley B. J. Alder (1980). Ground state of the electron gas by a stochastic method, *Physical Review Letters* **45**, 566.
[28] J. P. Perdew A. Zunger (1981). Self-interaction correction to density-functional approximations for many-electron systems, *Physical Review B* **23**, 5048.
[29] K. B. John P. Perdew, Matthias Ernzerhof (1996). Generalized gradient approximation made simple. *Physical Review Letters* **77**, 3865.
[30] J. P. Perdew, A. Ruzsinszky, G. I. Csonka, O. A. Vydrov, G. E. Scuseria, L. A. Constantin, X. Zhou, and K. Burke(2008). Restoring the density-gradient expansion for exchange in solids and surfaces, *Phys Rev Lett* **100**, 136406.
[31] C.G. Van de Walle, J. Neugebauer (2004). First-principles calculations for defects and impurities:Applications to III-nitrides, *Journal of Applied Physics* **95**, 3851.
[32] V. Kumar (2015). Structural analysis by rietveld method and its correlation with optical propertis of nanocrystalline zinc oxide, *Advanced Materials Letters* **6**, 139.
[33] S. Goel, N. Sinha, H. Yadav, A. J. Joseph, B. Kumar (2017). Experimental investigation on the structural, dielectric, ferroelectric and piezoelectric properties of La doped ZnO nanoparticles and their application in dye-sensitized solar cells, *Physica E: Low-dimensional Systems and Nanostructures* **91**, 72.
[34] P. Wei, (2012). First-principles study on La-doped ZnO used as transparent electrode for optoelectronic device, *International Journal of the Physical Sciences* **7**, 2174-2180.
[35] K. Harun, N. A. Salleh, B. Deghfel, M. K. Yaakob, A. A. Mohamad (2020). DFT + U calculations for electronic, structural, and optical properties of ZnO wurtzite structure: A review, *Results in Physics* **16**, 102829.

[36] X. Ma, Y. Wu, Y. Lv, Y. Zhu (2013). Correlation Effects on Lattice Relaxation and Electronic Structure of ZnO within the GGA+U Formalism, *The Journal of Physical Chemistry C* **117**, 26029.
[37] AM Prokofiev, A.I. Shelykh, B. T. Melekh (1996). Periodicity in the band gap variation of Ln_2X_3 (X = O, S, Se) in the lanthanide series, *Journal of Alloys and Compounds* **242**, 41.
[38] M.H. Huang, S. Mao, H. Feick, H. Yan, Y. Wu, H. Kind, E. Weber, R. Russo, P. Yang (2001). Room-temperature ultraviolet nanowire nanolasers. *Science* **292**, 1897.
[39] C. L. Dong, C. Persson, L. Vayssieres, A. Augustsson, T. Schmitt, M. Mattesini, R. Ahuja, C. L. Chang, and J.-H. Guo (2004). Electronic structure of nanostructured ZnO from x-ray absorption and emission spectroscopy and the local density approximation, *Physical Review B* **70**, 195325.